J. Astron. Space Sci. 23(4), 303–310 (2006)

ASPHERICAL DUST ENVELOPES AROUND OXYGEN-RICH AGB STARS

Kyung-Won Suh
Department of Astronomy and Space Science, Chungbuk National University, Cheongju 361-763, Korea
email: kwsuh@ast.chungbuk.ac.kr

(Received October 21, 2006; Accepted October 29, 2006)

ABSTRACT

We model the aspherical dust envelopes around O-rich AGB stars. We perform the radiative transfer model calculations for axisymmetric dust distributions. We simulate what could be observed from the aspherical dust envelopes around O-rich AGB stars by presenting the model spectral energy distributions and images at various wavelengths for different optical depths and viewing angles. The model results are very different from the ones with spherically symmetric geometry.

Keywords: circumstellar matter, stars: AGB and post-AGB, infrared: stars, dust: extinction, radiative transfer

1. INTRODUCTION

AGB stars are generally considered to be the final phase of stellar evolution before leaving the red giant branch and rapidly evolving into a planetary nebula. The shape of most planetary nebulae are known to be aspherical (bicones, tori, multiple arcs, and globules) as confirmed by many authors (e.g., Meixner 2004). This could imply that AGB stars may have aspherical dust envelopes around them. Various high angular resolution observations (Ragland et al. 2006, Monnier et al. 2004) of many AGB stars revealed departure from circular symmetry in the optical and near-infrared images.

Ragland et al. (2006) carried out a survey of AGB stars with the IOTA 3-telescope imaging interferometer at near-infrared wavelengths, searching for asymmetry in their flux distributions. They find that a major portion of AGB stars in the sample shows asymmetry from the observations. Polarimetric observations of AGB stars have shown that significant fraction of the stars show excessive intrinsic polarization (Johnson & Jones 1991, Jones & Gehrz 1990). These observations could be explained by aspherical shape of the dust envelopes around AGB stars.

Various mechanisms have been suggested to explain the deviation from symmetry, including large-scale convective cells, non-radial pulsation, binary companions, stellar rotation and uneven molecular opacity. But no serious consensus exists yet as to the convincing mechanism that would cause such asymmetry.

In this work, we perform the radiative transfer model calculations for axisymmetric dust distributions. We simulate what could be observed from the aspherical dust envelopes around O-rich AGB stars by presenting the model spectral energy distributions (SEDs) and images at various wavelengths for different optical depths and viewing angles.

2. MODEL CALCULATIONS

We use the dust radiative transfer code (2-dust) for an axisymmetric system by Ueta & Meixner (2003). The code was originally developed by Collison & Fix (1991). For this work, 61 radial grid points and a wavelength grid of 46 points were used. The radiation from a central hot source hits the inner part of the dust envelope around it and the dust grains redistribute the energy spectra continuously toward longer wavelength bands. We calculate the model SEDs and images for different viewing angles to the edge of the axisymmetric system.

Silicates are believed to be a major component of the dust grains in the envelopes around O-rich AGB stars. The SEDs of them are usually well fitted with amorphous (or dirty) silicates. Low mass-loss rate O-rich AGB (LMOA) stars with thin dust envelopes show the 10μm and 18μm emission features. And high mass-loss rate O-rich AGB (HMOA) stars with thicker dust envelopes show the absorbing features at the same wavelengths.

2.1 Central stars

For the central star, the luminosity is taken to be $1 \times 10^4 L_{\odot}$ and a stellar black body temperature of 2000 K for HMOA stars and 2500 K for LMOA stars is used. A change in the luminosity does not affect the shape of the output spectra, it only affects the overall energy output. A change in the blackbody temperature of the central star does affect the output spectra, especially for LMOA stars.

2.2 Dust envelope parameters

For dust opacity, we use the optical constants of amorphous silicate grains derived by Suh (1999). We use the warm dust opacity function for LMOA stars and the cold dust opacity function for HMOA stars. For simplicity, we assume that all silicate dust grains are spherical with a uniform radius of 0.1 μm and the bulk density is 3.0 g cm $^{-3}$.

The inner radius of the dust envelope (R_c) was chosen to produce the dust temperature at R_c is about 1000 K. After a few trials, we find the dust shell inner radius (R_c) at which the dust temperature (the inner shell dust temperature; T_c) becomes the desired one. The model SEDs are sensitively dependent on T_c. The temperature is not necessarily the same as the dust formation temperature depending on the physical condition of the pulsating AGB star (see Suh 2004).

For the dust density distribution, we use the equation 1 which is a simplified form of the one used in Ueta & Meixner (2003). For this work, we use the following parameters: B=2, A=9 and F=1 for all aspherical models. The density distribution is for a highly flattened dust shell. The pole-to-equator density ratio ($\rho_{\rm eq}/\rho_{\rm pole}$) is 10. For spherically symmetric models, we use B=2 and A=0.

$$\rho(r,\Theta) = \rho(R_c,\Theta)\left(\frac{r}{R_c}\right)^{-B}\left[1 + A(1-\cos\Theta)^F\right]. \quad (1)$$

For a given polar angle (Θ), we assume that the dust envelope density distribution is continuous ($\rho \propto r^{-2}$) in large scale from the inner radius of the dust envelope (R_c) to the outer radius which is always taken to be 1000 R_c. Although AGB stars are pulsating, the outer region of the dust shells show constant expansion velocity ($v_{exp} \sim 10-30$ km/sec). This implies that almost constant mass-loss rate is maintained for a time scale larger than the pulsation period (e.g., Herman & Habing 1985).

The dust optical depth at 10 μm(τ_{10}) in the equatorial direction ($\Theta = 90^\circ$) is the adjustable parameter that determines the overall thickness of the dust envelope and the mass-loss rate. For this work, we use τ_{10} = 0.1 for a typical LMOA star and $\tau_{10} = 30$ for a typical HMOA star.

Table 1. Model parameters.

Class	T_*	R_c (R_*)	τ_{10}(equator)	τ_{10}(pole)	$\dot{M}_{dust}$ ($M_\odot/yr$)	T_c (equator)	T_c (pole)
LMOA (spherical)	2500	7.7	0.1	0.1	5.2×10^{-9}	875	875
LMOA (aspherical)	2500	7.7	0.1	0.01	2.8×10^{-9}	868	863
HMOA (spherical)	2000	4.9	30	30	1.4×10^{-6}	1214	1214
HMOA (aspherical)	2000	4.9	30	3	7.6×10^{-7}	1060	993

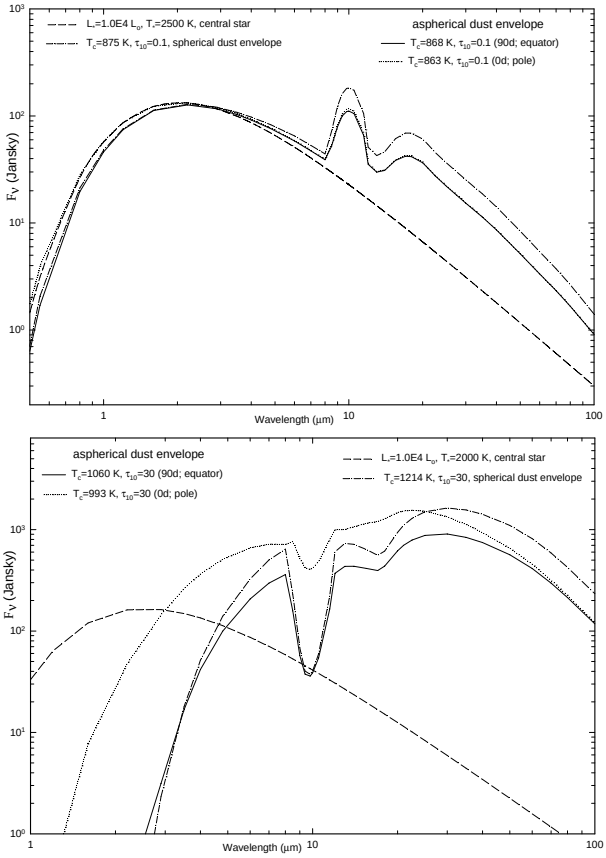

Figure 1. Model SEDs for O-rich AGB stars (τ_{10}=0.1, 30).

3. RESULTS AND DISCUSSION

The distance to the all model objects is set to be 1 kpc. The inner radius of the dust envelope (R_c) was chosen to be 19 mas. Table 1 lists model parameters. We assume that $v_{exp} = 15$ km/sec to calculate the dust mass-loss rate ($\dot{M}_{dust}$).

Figure 1 shows model SEDs of the spherical and aspherical dust envelopes around the LMOA and HMOA stars. For aspherical dust envelope models, the model SEDs are different depending

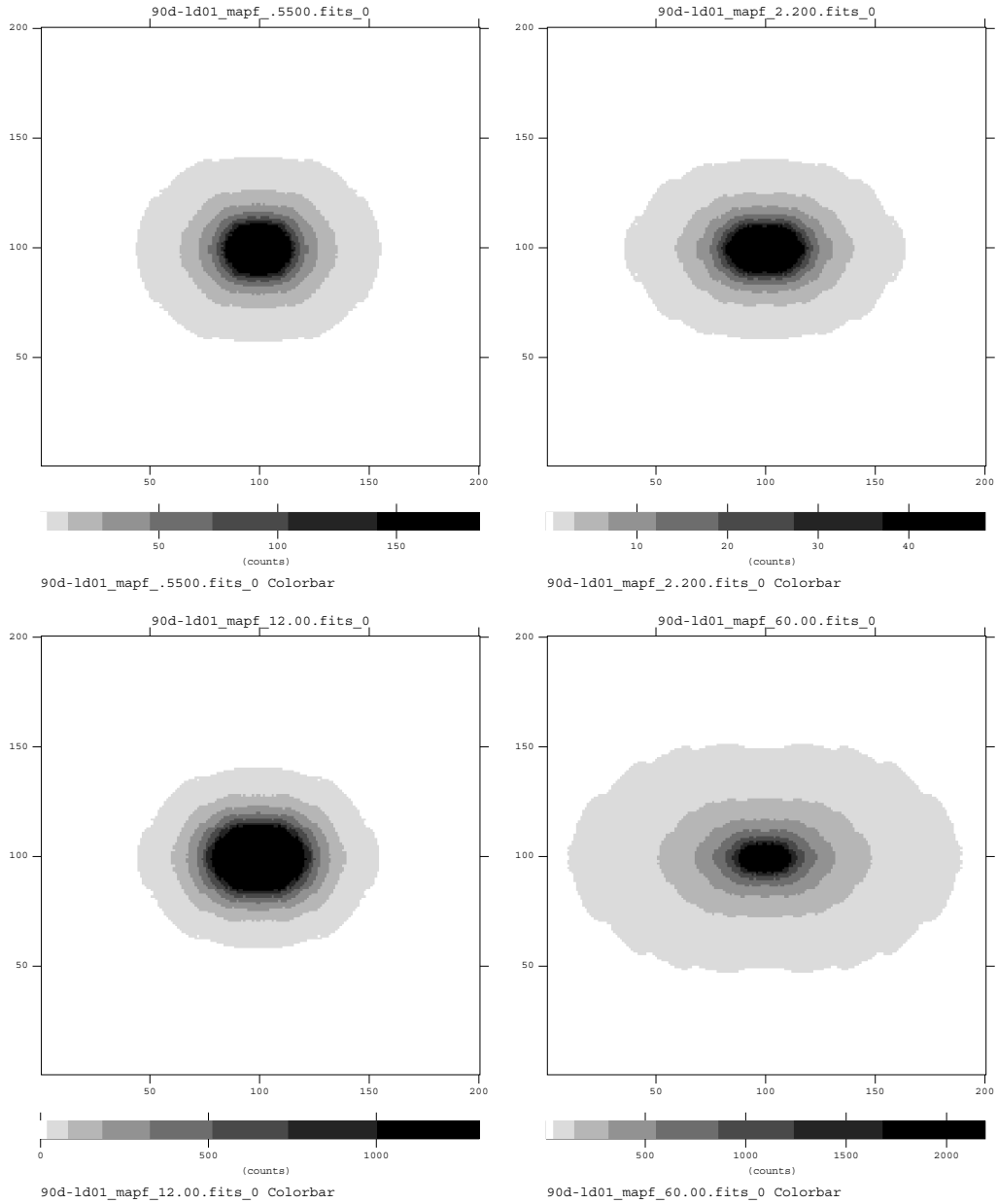

Figure 2. Edge-on view model images of the aspherical dust envelope at 0.5, 2.2, 12 and 60μm for the LMOA star (τ_{10}=0.1). The model image surface brightness is in units of mJy/arcsec^2.

on the viewing angle (i). The SED for the edge on view ($i = 90^\circ$) shows largest redistribution of the central flux. The difference of the SEDs depending the viewing angle is much larger for HMOA stars. The inner shell dust temperature (T_c) is higher for spherical model for the isotropic

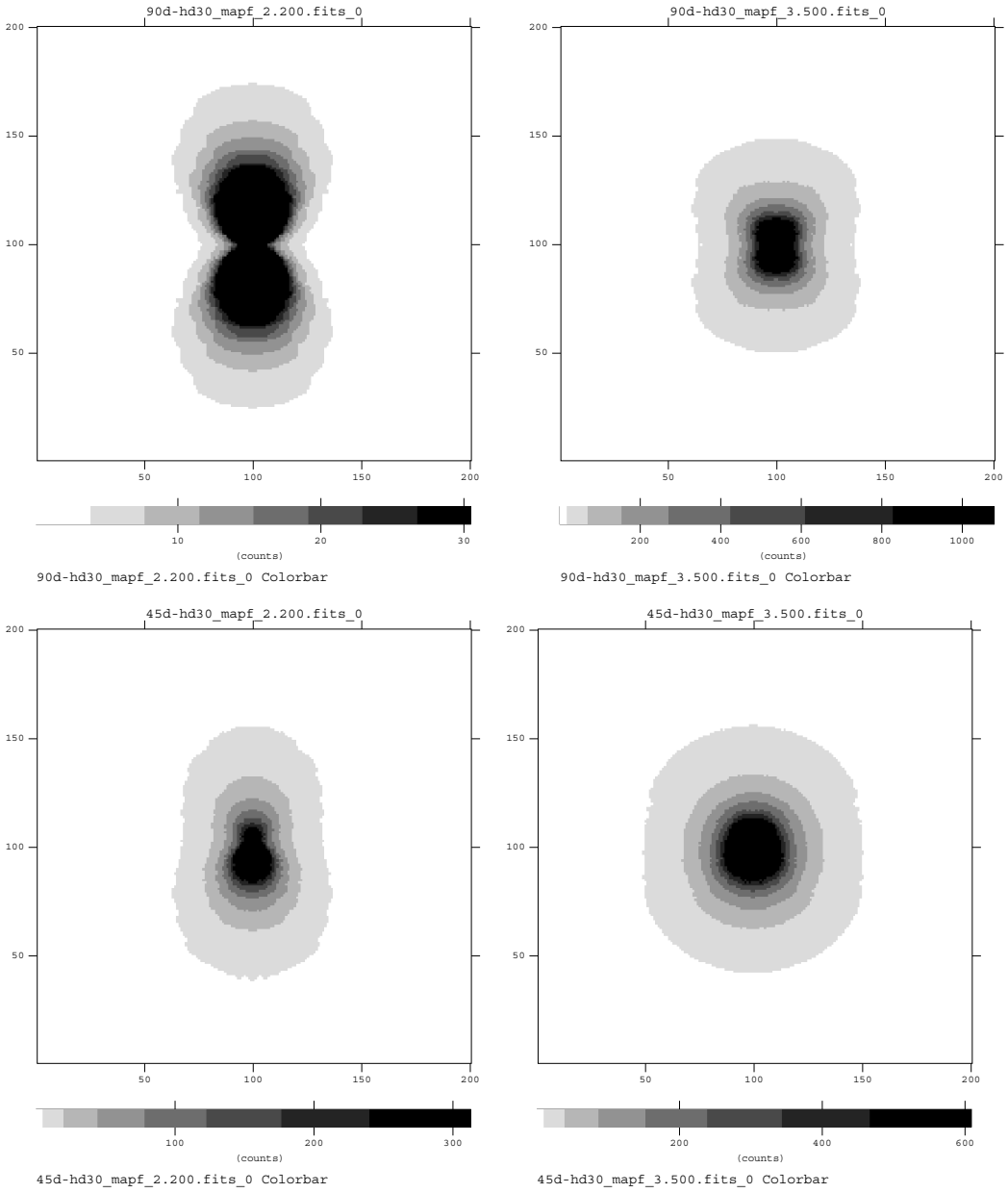

Figure 3. Edge-on (upper panels) and $i = 45^{\circ}$ (lower panels) view model images of the aspherical dust envelope at 2.2 and 3.5 μm for the HMOA star (τ_{10}=30). The model image surface brightness is in units of mJy/arcsec^2.

greenhouse effect. For aspherical models, T_c in the equatorial direction is higher than the one in the polar direction because of the dust density difference.

Figure 2 through Figure 4 show the model images of the O-rich AGB stars with aspherical dust

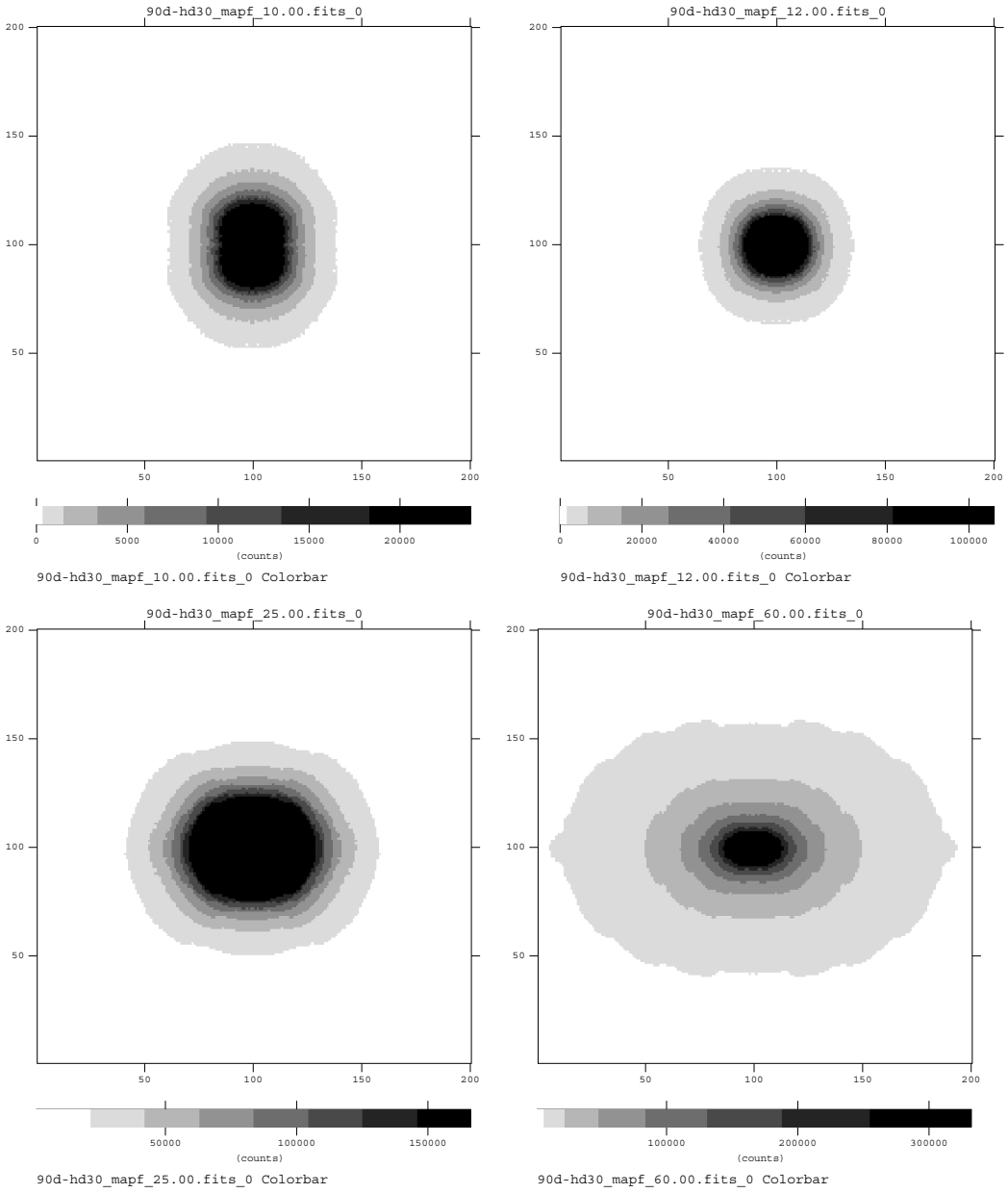

Figure 4. Edge-on view model images of the aspherical dust envelope at 10, 12, 25 and 60 μm for the HMOA star (τ_{10}=30). The model image surface brightness is in units of mJy/arcsec^2.

envelopes. In the model image figures (200×200 pixels), each pixel corresponds to 20 mas at all wavelengths. If the distance of an object is x kpc, the actual pixel resolution of the model image will be $\frac{20}{x}$ mas. Note that the size of the stellar surface is much less than a pixel of the images (see Table

1). The model image surface brightness is presented in units of mJy/arcsec^2.

The model images of the aspherical dust envelopes for the LMOA star are shown in Figure 2. The edge on view ($i = 90°$) model images at all wavelengths show similarly flattened shapes in equatorial direction. The image at 60μm shows the most flattened shape which is similar to the real dust distribution. The equatorial asymmetry would be easily detectable with enough angular resolution.

The model images for the HMOA star are very different at different wavelengths. Figure 3 shows the model images of the aspherical dust envelopes for the HMOA star at near-IR wavelengths. The shape of the edge on view model images ($i = 90°$) is bipolar. Even when $i = 45°$, the polar deviation from symmetry is noticeable. This is very different from the real dust density distribution which is asymmetric in equatorial direction.

Figure 4 shows the model images of the aspherical dust envelopes for the HMOA star at longer IR wavelengths. They show slightly polar oriented shape at 10μm and almost circular (symmetric) shape at 12μm. The model images at far IR wavelengths (25 and 60μm) show similarly flattened shapes. The image at 60μm is very bright and show noticeable equatorial asymmetry.

The observed departures from circular symmetry have been interpreted either in terms of elliptical distortions or an otherwise symmetric photosphere or circumstellar envelope containing localized features (Ragland et al. 2006, Mauron & Huggins 2006) for AGB stars. The model images at different wavelengths show very different shapes for HMOA stars. Therefore, it would be difficult to detect the departure from circular symmetry from the observed images in some wavelength ranges (e.g., $5 - 30\mu$m) for HMOA stars.

4. CONCLUSIONS

We have modeled the aspherical dust envelopes around O-rich AGB stars. We performed the radiative transfer model calculations for axisymmetric dust distributions. We have simulated what could be observed from the aspherical dust envelopes around O-rich AGB stars by presenting the model SEDs and images at various wavelengths for different optical depths and viewing angles. The model results are very different from the ones with spherically symmetric geometry. We expect that the results would be helpful to make plans to perform new high resolution observations of O-rich AGB stars and understand the data.

ACKNOWLEDGEMENTS: This work was supported by Korea Research Foundation Grant funded by Korea Government (MOEHRD, Basic Reasearch Promotion Fund; KRF-2005-015-C00194).

REFERENCES

Collison, A. J. & Fix, J. D. 1991 ApJ, 368, 545
Herman, J. & Habing, H. J. 1985, Physics Report, 124, 255
Johnson, J. J. & Jones, T. J. 1991, AJ, 101, 1735
Jones, T. J. & Gehrz, R. D. 1990, AJ, 100, 274
Mauron, N. & Huggins, P. J. 2006, A&A, 452, 257
Meixner, M. 2004, in ASP Conf. Ser. 313, Asymmetrical Planetary Nebulae III, eds. M. Meixner, J. H. Kastner, B. Balick & N. Soker (San Francisco: ASP), 24
Monnier, J. D. et al. 2004, ApJ, 605, 436
Ragland, S. et al. 2006, ApJ, in press
Suh, K. -W. 1999, MNRAS, 304, 389

Suh, K. -W. 2004, ApJ, 615, 485
Ueta, T. & Meixner, M. 2003, ApJ, 586, 1338